2015 International Conference on Condition Assessment Techniques in Electrical Systems (CATCON)

Automatic Detection of Powerlines in UAV Remote Sensed Images

Ramesh KN[a], A Sreenivasa murthy[a]
[a]Department of Electronics and Communication
UVCE, Bangalore, India

Senthilnath J[b], SN Omkar[b]
[b]Department of Aerospace Engineering, IISC
Bangalore, India

***Abstract*— Powerline detection is one of the important applications of Uninhabited Aerial Vehicle (UAV) based remote sensing. In this paper, powerlines are detected from UAV remote sensed images. The images are acquired from a Quad rotor UAV fitted with a GoPro® camera. In the proposed method pixel intensity-based clustering is performed followed by morphological operations. K-means clustering is applied for clustering. The number of clusters to be used in k-means clustering is automatically generated using Davies-Bouldin (DB) index. Further, the clustered data is processed to improvise the extraction using mathematical morphological operations. Performance of powerline extraction is analysed using confusion matrix method. In the observed results of powerline extraction using DB index, evaluation features derived from confusion matrix is close to one, indicating good classification.**

Keywords*— *UAV; Powerline Extraction; Davies-Bouldin index; k-means

I. INTRODUCTION

Power line inspection is a critical requirement in the maintenance of electric power transmission infrastructure. Conventional manual power line corridor inspection processes are labor intensive, time consuming and expensive. Ineffective surveillance could lead to loss of reliability of electricity transmission and introduce safety risks. Currently, most electricity companies use calendar based ground inspection. However, calendar based inspection by linesman is labour intensive, time consuming and expensive. It also leads to accessible areas being inspected more frequently as compared to hard to access areas.

Powerline corridor monitoring application using remote sensing has great potential [2]. Remote sensing from a manned aircraft platform is an option but they are limited by their high operational costs [3]. To overcome this challenge, remote optical sensors mounted on unmanned aerial vehicles (UAVs) provide a cheap and flexible option to acquire spatial data from powerline corridors. They meet the requirements of high spatial and temporal resolutions.

Several researchers [4-8] have used UAV based imaging sensors to detect powerlines from diverse backgrounds. In the literature, edge detection followed by straight line detection is one of the commonly used method for detecting power lines in an image. Li et al. [1] developed a simplified pulse coupled neural network model which removed the back ground noise and generated edge maps. Further an improved Hough transform was used by performing knowledge-based line clustering in Hough space to refine the detection results. Liu et al. [4] used an algorithm based on a statistical analysis of the data to segment object points from ground points in LIDAR intensity data. Hough transform was then employed to discriminate powerlines from other objects (i.e. vegetation). Yan et al. [5] used line detector mask to detect powerline pixels followed by ratio line detectors for linear object extraction. Radon transform was used to trace candidate lines. Later, Kalman filter was used to fill out the broken lines. This detector assumes that the lines are parallel. Ceron et al. [6] used a method for powerline detection based on computer graphics algorithms. The algorithm used geometric relationships that are inherent to the circle symmetry. The method detected line segments that were linked in a posterior stage. For the detection, Canny and steerable Filters were used. The classical methods of edge detection followed by line detection are sensitive to noise due to complex and irregular ground coverage in aerial images, hence impacting the quality performance of the power line detection algorithms [1].

Light Detection and Ranging (LIDAR) based remote sensing is an other option. LIDAR is a remote sensing technology that measures distance by illuminating a target with a laser and analyzing the reflected light. LIDAR provides elevation and terrain models which can be used to identify linear features similar to powerlines such as fences. Jwa et al. [7] used LIDAR 3D point cloud data in which voxel classification was used to cluster similar features. Li and Walker et al. [8] performed statistical analysis of 3 point cloud intensity data to classify terrain and objects. Later it was mapped into 2D plane and Hough transform was applied to detect lines. One of the main limitations of using LIDAR in UAVs is the size of the sensor and its power requirements which make them too heavy for the UAVs. There are small LIDAR systems available in the market however their quality does not match their full size LIDARs.

In this paper we propose a powerline extraction method that involves clustering followed by mathematical morphology operations. The number of clusters (k) to be used for

978-1-4673-7748-5/15/$31.00 ©2015 IEEE

clustering is determined by the DB index method [9] [10]. K-means clustering to partition the image in to k clusters [11] [12] [13]. K-means clustering is performed on the intensity values of the pixels using Euclidian distance metric. Agglomeration of clusters from k clusters to two clusters (power line and non power line) is carried out by exploiting the reflectance characteristics of power lines in UAV images. Further processing is performed to improvise the extraction. The non powerline pixels are filtered out using mathematical morphological operations. The morphological operations includes a combination of skeletonisation, region growing and determining Shape Index (SI) and Density index (DI) of clustered regions [14] [15]. SI and DI uses the geometric properties of the regions to segment the linear powerline regions. Performance of powerline detection is evaluated by computing the evaluation feature parameters - precision, recall, accuracy and F-measure derived from the confusion matrix.

II. POWERLINE EXTRACTION STEPS

The powerline image dataset is acquired through UAV remote sensing. A Quadrotor UAV fitted with a GoPro® camera is flown over a powerline corridor and the video is recorded. Image frames representing the powerline is extracted from the video. The extracted image is used for processing. It can be observed from Fig. 1. that the image is acquired at an oblique aerial orientation as opposed to a nadir orientation, This is to ensure that a longer length of the powerline is captured in the image.

Powerline extraction comprises seven steps S1 through S7, as shown in Fig 2. The number of clusters to be used for the image datset clustering is automatically determined using DB index [9] [10] [17], in step 1. Clustering is performed in step 2 to partition the dataset based on the intensity values. Novel hierarchical method that exploits the unique reflectance characteristics of the powerlines are used to merge the partitions from 4 clusters to 2 clusters (powerline and non powerline pixels). In step 3 , the partitioned image is prepared for further processing. To improvise the clustering results, skeletonisation is performed in step 4. Skeletonisation extracts the line features in the image, the extracted lines are however not continuous. The extracted line features are transformed into linear lines using region growing method, in step 5. The extraction is further improvised by eliminating the non powerline pixel regions. Step 6 is a novel method of extracting line features of the regions using SI and DI. The line features are extracted at the end of step 6. At the end of step 6 residual non power line pixel regions are observed, to eliminate these regions, the sequence of steps s4, s5 and s6 are repeated to improve the extraction further. Hough transform is used in step 7 to draw lines from the extracted line features to be superimposed on the original image to highlight the extracted lines. It must be noted that the line features are already extracted at the end of step 6. Hough transform is used in step 7 to draw the lines to be superimposed on the original image, to provide a visual view of the extracted power lines.

Fig. 2. Original image

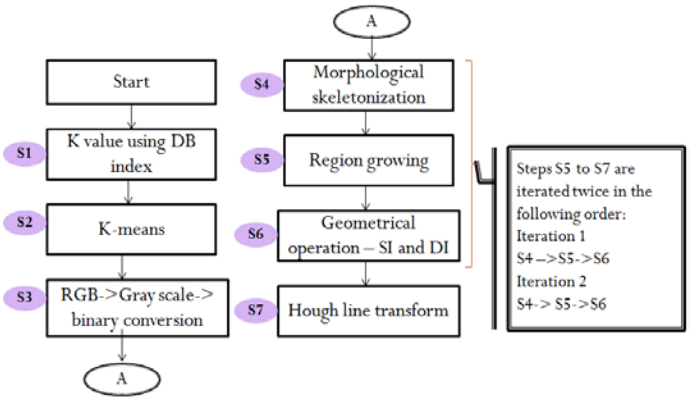

Fig. 1. Powerline extraction steps

DB index [17] is a statistical method to reduce the intra cluster distance and increase the inter cluster distance. DB Index takes into consideration the inter cluster distance and the intra cluster distance where intra cluster distance should be less, signifying tight and compact clusters and inter cluster distance should be more, signifying well separated clusters' distribution. The mean distance of points belonging to a specific cluster C_k or the intra cluster distance given by [17]

$$\delta_k = \frac{1}{n_k}\sum_{i\in I_k}\left\|M_i^{\{K\}} - G^{\{K\}}\right\| \quad (1)$$

where n_k is the number of points associated with the cluster k, $M_i^{\{K\}}$ is the i^{th} point of cluster k and $G^{\{K\}}$ is the centroid of the cluster k .

Also $\Delta_{KK'} = d(G^{\{K\}}, G^{\{K'\}}) = \left\|G^{\{K'\}} - G^{\{K\}}\right\|$

Where, $\Delta_{KK'}$ is the inter cluster distance between cluster centers $G^{\{K\}}$ and $G^{\{K'\}}$ of clusters C_k and $C_{K'}$. The values of δ_k and $\Delta_{KK'}$ are calculated for a range of values for k. DB index d, a ratio of intra cluster to inter cluster separation is given by

$$d = \frac{1}{K}\sum_{k=1}^{K}\max_{k'\neq k}\left(\frac{\delta_k + \delta_{k'}}{\Delta_{kk'}}\right) \quad (2)$$

The DB index for a range of k values from 2 to 20 is shown in Fig 3. A low value of DB index indicates good separation hence the k value corresponding to the lowest DB index is the right choice of k value.

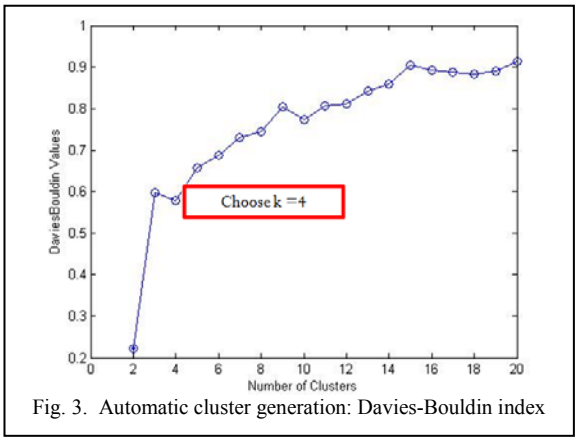

Fig. 3. Automatic cluster generation: Davies-Bouldin index

From Fig 3, it can be seen that the lowest DB index value occurs for a value of *k* value of 2. And the next lowest value occurs for a *k* value of 4. *k* value of 2 indicates clustering of actual required class of power line and non power line pixels which does not provide good clustering performance. Hence the next minimum of DB index, for the given image distribution which occurs for a k value of 4 is chosen for K-means clustering.

B. K-means clustering

K-means clustering [11] [12] [13] is a popular unsupervised parametric algorithm in which the number of clusters *k* is known a priori. The objective function is the square of the sum of errors of the distance metric which is the Euclidian distance in the given study. The minima of the objective function is chosen as the cluster centre. The objective function is given by

$$J(k) = \sum_{k=1}^{K} \sum_{x_i \in c_k} \left\| x_i - c_k \right\|^2 \tag{3}$$

where $\|.\|$ is the distance metric in Euclidian space, c_k is the k^{th} cluster centre given by $c_k = \sum_{i \in c_k} \frac{x_i}{n_k}$ and n_k is the number of data points in the cluster k. n_k is determined using the minima of the objective function $J(k)$.

It can be seen from Fig. 3 that the number of clusters automatically generated using DB index is 4. However the objective is to classify powerline and non powerline pixels. The number of clusters need to be agglomerated to 2. To agglomerate from 4 clusters to 2 clusters, we exploit the reflectance characteristics of the powerline and its back ground. The powerline pixels are brighter pixels and the back ground pixels are vegetation and land mass which are darker pixel values. Two partitions which are closer to dark intensity values are mapped to black pixel values of 0. The resultant image is converted from grey to binary. The result of this step is shown in Fig. 4.

Fig. 4. Clustered and binarised

C. Mathematical morphological skeletonisation

Morphological skeleton is a one pixel wide caricature that summarizes the overall shape, size, orientation and association of a geometric structure from which inferences can be drawn [16]. The skeletonisation of a geometric structure can be mathematically defined as [16]

$$Sk_n(X) = ((X \Theta nB) \setminus (X \Theta nB) oB) \tag{4}$$

where n =0,1,2,….,N. $Sk_n(X)$ denotes the n^{th} skeletal subset of set (X), B is the structuring element, Θ is an erosion transformation , ' \' is a logical difference operator and o is an open transformation given by

$$XoB = ((X \Theta B) \oplus B) \tag{5}$$

In the equation (4), subtracting from the eroded versions of set X , their opening by B retains only the angular points. The union of all such possible points results in $Sk(X)$, the skeletal of set (X), given by

$$Sk(X) = \bigcup_{n=0}^{N} Sk_n(X) \tag{6}$$

In Fig 4, It can be observed that the far end of power line in the image has merged pixel and non pixel regions. Skeletonisation extracts the caricature of the power lines as shown in Fig. 5.

D. Region growing, Shape index (SI) and Density index (DI)

The skeletal divides the powerline and non power linear regions, however the power line regions in the image contain disconnected or separated pixels. Region growing is used to create homogeneous regions in the image . Region growing involves growing pixels by comparing all unallocated neighbouring pixels to the region. In this study region growing is used to identify and bridge unconnected pixels in the powerline.

Shape Index (SI) is a geometrical parameter given by

$$SI = P / (4 * \sqrt{A}) \tag{7}$$

where P represents the perimeter of the object (i.e. the number of pixels on the boundary of the object) and A represents the area of the object.

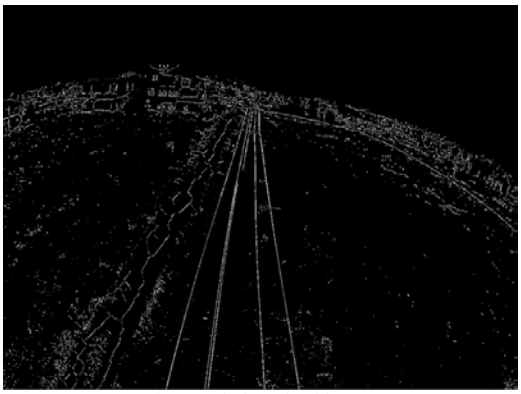

Fig. 5. Skeletonised image

Density Index (DI) is given by

$$DI = \sqrt{A} / (1 + v) \quad (8)$$

Where v is given by

$$v = \sqrt{Var(X) + Var(Y)} \quad (9)$$

Var(X) represents the variance of x-coordinates of all pixels and *Var(Y)* represents the variance of y-coordinates of the region. Equation 9. approximates the radius of the region [14] [15].

A high SI indicates line segments and a high DI indicates large area objects. Since the powerlines are relative long and thin objects, perimeter of the powerline regions are relatively higher for power lines than that of non powerline regions. Hence, a large SI and low DI is chosen to select the powerlines and exclude non powerline regions. A white pixel indicates a powerline pixel and a non white pixel indicates a non-powerline pixel. The SI value chosen is 0.6 and DI value chosen is 0.3. Result of region growing is shown in Fig. 6 and the results of SI and DI operations are shown in Fig. 7.

Further, the extracted lines are super imposed on the original image (Fig. 1) to high light the extracted lines and obtain the final blended image, as shown in Fig. 8.

E. Performance evaluation

Confusion matrix is used to evaluate the performance of classification. The parameters computed are True positive (TP), True Negative (TN), False Positive (FP) and False (Negative). Further, the following evaluation features are obtained [18] [19].

Precision, P = TP/(TP+FP) (10)

Recall, R = TP/(TP+FN) (11)

Accuracy = TP + TN /(TP+FP+FN+TN) (12)

F-measure , F = 2PR/(P+R) (13)

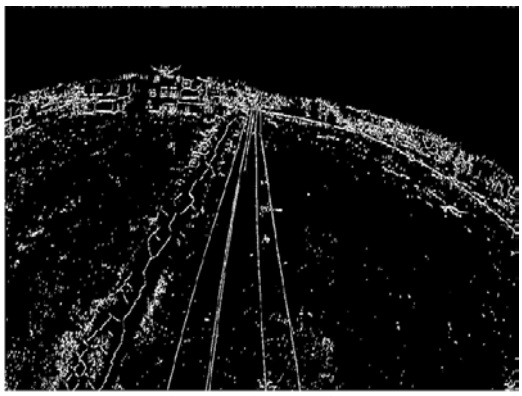

Fig. 6. Region growing

The confusion matrix is tabulated in Table 1. and the evaluation features obtained from the confusion matrix is tabulated in Table 2.

Table 1
Confusion matrix

		Ground truth, actual	
Predicted, extracted		Number of powerline pixels	Number of non-powerline pixels
	Number of powerline pixels	1217831 (TP)	1883 (FP)
	Number of non-powerline pixels	2664(FN)	6422(TN)

Table 2
Evaluation features

Feature	**Metric**
Precision	99.85%
Recall	99.78%
Accuracy	99.63%
F-measure	99.81%

For a good classifier all the evaluation features will be close to 100% which is true in the observed results hence signifying good classification.

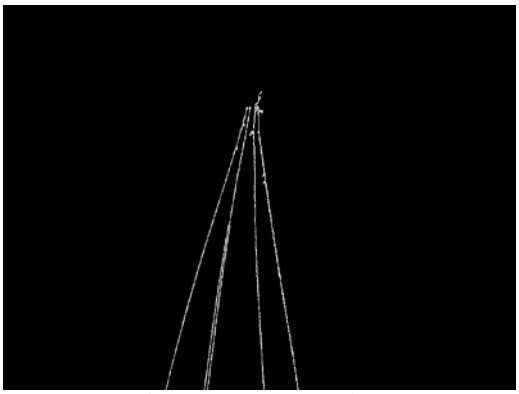

Fig. 7. Geometric operations

Fig. 8. Final blended image

III. CONCLUSION AND DISCUSSION

This work demonstrates successful detection of powerlines in an aerial image acquired from a Quadrotor UAV fitted with a high spatial resolution camera. The results show good quality extraction both from a visual perspective and from the performance metrics. The results are encouraging. As next steps the same algorithm can be extended to extract powerlines from aerial images acquired at different angles. Further the UAV payload can carry an altimeter to capture the altitude of acquired image which can be used to calculate the physical area under each image extent and hence compute the length of the power lines in every image. The experiments can be extended to extraction in stitched images to cover larger lengths of power lines.

Acknowledgment

The authors would like to thank the anonymous reviewers for their comments and suggestions. We would also like to thank Gautham Anand from IISc, for providing the aerial video. We would like to express our gratitude to Saurab Buttan for his help in region growing sub step.

References

[1] Li, Z., Liu, Y., Walker, R., Hayward, R., & Zhang, J. (2010). Towards automatic power line detection for a UAV surveillance system using pulse coupled neural filter and an improved Hough transform. Machine Vision and Applications,21(5), 677-686.

[2] Mu, C., Yan, Q., Feng, Y., Cai, J., & Yu, J. (2009, October). Overview of powerlines extraction and surveillance using remote sensing technology. In *Sixth International Symposium on Multispectral Image Processing and Pattern Recognition* (pp. 74981M-74981M). International Society for Optics and Photonics.

[3] Wang, B., Chen, X., Wang, Q., Liu, L., Zhang, H., & Li, B. (2010, October). Power line inspection with a flying robot. In *Applied Robotics for the Power Industry (CARPI), 2010 1st International Conference on* (pp. 1-6). IEEE.

[4] Liu, Y., Li, Z., Hayward, R., Walker, R., & Jin, H. (2009, December). Classification of airborne lidar intensity data using statistical analysis and hough transform with application to power line corridors. In Digital Image Computing: Techniques and Applications, 2009. DICTA'09. (pp. 462-467). IEEE.

[5] Yan, G., Li, C., Zhou, G., Zhang, W., & Li, X. (2007). Automatic extraction of power lines from aerial images. Geoscience and Remote Sensing Letters, IEEE, 4(3), 387-391.

[6] Ceron, A., Mondragon, B., Ivan, F., & Prieto, F. (2014, May). Power line detection using a circle based search with UAV images. In Unmanned Aircraft Systems (ICUAS), 2014 International Conference on (pp. 632-639). IEEE.

[7] Jwa, Y., Sohn, G., & Kim, H. B. (2009). Automatic 3d powerline reconstruction using airborne lidar data. Int. Arch. Photogramm. Remote Sens, 38, 105-110.

[8] Li, Z., Walker, R., Hayward, R., & Mejias, L. (2010, October). Advances in vegetation management for power line corridor monitoring using aerial remote sensing techniques. In Applied Robotics for the Power Industry (CARPI), 2010 1st International Conference on (pp. 1-6). IEEE.

[9] Senthilnath, J., Kumar, D., Benediktsson, J. A., & Zhang, X. (2015). A novel hierarchical clustering technique based on splitting and merging. International Journal of Image and Data Fusion, (ahead-of-print), 1-23.

[10] Tarabalka, Y., Benediktsson, J. A., & Chanussot, J. (2009). Spectral–spatial classification of hyperspectral imagery based on partitional clustering techniques. *Geoscience and Remote Sensing, IEEE Transactions on*, *47*(8), 2973-2987.

[11] MacQueen, J. (1967, June). Some methods for classification and analysis of multivariate observations. In Proceedings of the fifth Berkeley symposium on mathematical statistics and probability (Vol. 1, No. 14, pp. 281-297).

[12] Savaresi, S. M., & Boley, D. L. (2001, April). On the performance of bisecting K-means and PDDP. In SDM (pp. 1-14).

[13] Rollet, R., Benie, G. B., Li, W., Wang, S., & Boucher, J. M. (1998). Image classification algorithm based on the RBF neural network and K-means.International Journal of Remote Sensing, 19(15), 3003-3009.

[14] Senthilnath, J., Bajpai, S., Omkar, S. N., Diwakar, P. G., & Mani, V. (2012). An approach to multi-temporal MODIS image analysis using image classification and segmentation. *Advances in Space Research*, *50*(9), 1274-1287.

[15] Song, M., & Civco, D. (2004). Road extraction using SVM and image segmentation. *Photogrammetric Engineering & Remote Sensing*, *70*(12), 1365-1371.

[16] Sagar, B. S. D. (2013). Mathematical morphology in geomorphology and GISci. CRC Press.

[17] Davies, D. L., & Bouldin, D. W. (1979). A cluster separation measure. Pattern Analysis and Machine Intelligence, IEEE Transactions on, (2), 224-227.

[18] Omkar, S., Sivaranjani, V., Senthilnath, J., & Mukherjee, S. (2010). Dimensionality reduction and classification of hyperspectral data. International Journal of Aerospace Innovations, 2(3), 157-164.

[19] Suresh, S., Sundararajan, N., & Saratchandran, P. (2008). Risk-sensitive loss functions for sparse multi-category classification problems. Information Sciences, 178(12), 2621-2638.